Abdominal Radiology (2025) 50:4553–4562
https://doi.org/10.1007/s00261-025-04865-4

RESEARCH

Preoperative prediction of pancreatic neuroendocrine tumors grade based on computed tomography, magnetic resonance imaging and endoscopic ultrasonography

Yu Xie[1] · Elyar Abaydulla[1] · Song Zhang[2] · Haobai Liu[1] · Hexing Hang[1] · Qi Li[3] · Yudong Qiu[1] · Hao Cheng[1]

Received: 18 December 2024 / Revised: 24 February 2025 / Accepted: 28 February 2025 / Published online: 19 March 2025

Abstract

Purpose To establish a preoperative prediction model for pathological grade of PanNETs based on computed tomography (CT), magnetic resonance imaging (MRI) and endoscopic ultrasonography (EUS).

Methods Clinical data of 58 patients with pathologically confirmed PanNETs were included in this retrospectively study and they were divided into grade 1 and grade 2/3. CT, MRI and EUS images were collected within one week before surgery. A clinical predictive model based on the independent clinical risk factors and significant radiological features was established. The area under receiver operating characteristic curve (AUC) was performed to assess the model.

Results Gender, pancreatic duct dilatation (PDD) and portal enhancement ratio (PER) were the independent predictors for PanNETs grading ($P < 0.05$). PanNETs grade 1 and grade 2/3 had statistical difference in elastography score ($P = 0.001$). The combination of gender, PDD and PER had better predictive efficiency than each of these three predictors alone, with a high AUC of 0.925. The elastography score also achieved an AUC of 0.838.

Conclusion We proposed a comprehensive model based on preoperative CT, MRI and EUS to predict grade 1 and grade 2/3 of PanNETs and better informs clinicians on individualized diagnosis and treatment of patients with PanNETs.

✉ Yudong Qiu
yudongqiu510@163.com

✉ Hao Cheng
ch3320323@163.com

Yu Xie
maine371@163.com

Elyar Abaydulla
18999050469@163.com

Song Zhang
15951987557@163.com

Haobai Liu
liuhb0326@163.com

Hexing Hang
dg20350054@smail.nju.edu.cn

Qi Li
liqi0967@163.com

[1] Department of Pancreatic and Metabolic Surgery, Nanjing Drum Tower Hospital, Affiliated Hospital of Medical School, Nanjing University, Nanjing, China

[2] Department of Gastroenterology, Nanjing Drum Tower Hospital, Affiliated Hospital of Medical School, Nanjing University, Nanjing, China

[3] Department of Pathology, Nanjing Drum Tower Hospital, Affiliated Hospital of Medical School, Nanjing University, Nanjing, China

Graphical Abstract

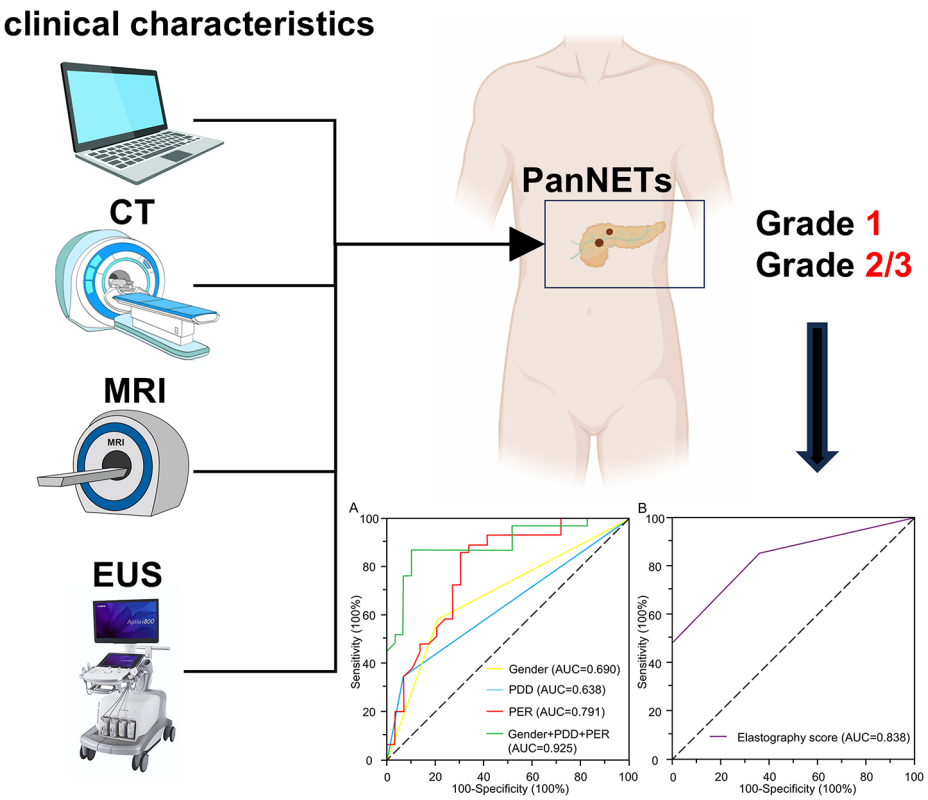

Keywords Pancreatic neuroendocrine tumors · Pathological grade · Computed tomography · Magnetic resonance imaging · Endoscopic ultrasonography

Introduction

Pancreatic neuroendocrine tumors (PanNETs) are a highly heterogeneous group of tumors, accounting for approximately 7% of all neuroendocrine neoplasm (NEN), with an incidence rate of 0.8 per 100,000 people [1]. According to the universal classification framework for neuroendocrine tumors proposed by the International Agency for Research on Cancer-World Health Organization (IARC-WHO), PanNETs are divided into grade 1, grade 2, grade 3 and Pancreatic neuroendocrine carcinomas (PanNECs) according to the number of mitotic rate and the Ki-67 proliferation index [2]. PanNECs typically have poorly differentiated morphological features and Ki-67 index of >50% [3]. The treatment selection of PanNETs is closely related to pathological grade, and whether the operation is considered and the choice of operation methods depend on the size, location, histopathological grade and stage of the tumor [4]. Recent studies have shown that the pathological grade of PanNETs has a great correlation with their prognosis. The 5-year survival rates of G1, G2 and G3 PanNETs were 79.54%, 66.88% and 22.53%, respectively [5]. Therefore, accurate preoperative prediction of pathological grade is of great significance for the prognostic assessment and treatment decision of PanNETs [6].

Imaging examination is an important means for the diagnosis, localization, staging and efficacy evaluation of PanNETs [7]. Common imaging examinations include computed tomography (CT), magnetic resonance imaging (MRI) and endoscopic ultrasonography (EUS). Multiphasic enhanced CT, as the preferred imaging examination for most patients with PanNETs, plays a crucial role in the qualitative and differential diagnosis of tumor [8, 9]. Meanwhile, the combination of imaging methods based on enhanced CT image features and patients' clinical information have high accuracy in predicting the pathological grade of PanNETs [10]. However, CT performs poorly in diagnosing small-sized PanNETs [11]. A recent study showed that more than 68% of PanNETs with diameter less than 10 mm and 15% of PanNETs with diameter between 11 and 20 mm could not be detected by CT [12]. MRI is also an effective mean to diagnose, differentiate and evaluate PanNETs. It is a suitable alternative method for CT detection and characterization of lesions, and it is a good choose when CT manifestations are

ambiguous or uncertain [11]. Also, MRI can be used as a supplementary means of CT examination because it has a high detection rate of PanNETs liver metastasis and lymph node metastasis with smaller maximum diameter [13]. EUS can provide more insights and access for PanNETs, and play a comprehensive role in positioning, staging, confirming and treating PanNETs [14]. EUS can observe the pancreas and its surrounding structures in detail, especially in the detection of small lesions (2–5 mm in diameter) with a diagnostic sensitivity of 86-89%, which is better than CT and MRI [15]. At present, EUS-guided fine needle aspiration (EUS-FNA) is a more accurate method to obtain the pathological grade of PanNETs before surgery [16]. However, due to the random selection of the biopsy sites and the limited size of the tissue obtained, the results of needle biopsy may not accurately reflect the proliferative status of the entire tumor [17]. Meanwhile, the invasive nature of needle biopsy and the risk of puncture failure should not be ignored [18].

Considering the disadvantages of the single imaging method, the combination of multiple examination methods may improve the accuracy of PanNETs diagnosis and provide more effective information for the formulation of treatment plan and follow-up plan. However, few studies have combined two or three imaging methods to predict the pathological grade of PanNETs before surgery. Hence, the purpose of this study was to build a comprehensive model based on CT, MRI, EUS features and clinical factors to predict the pathological grade of PanNETs before operation, and provide important guideline for clinical decision-making.

Materials and methods

Patient selection

This retrospective study has been approved by the local institutional review board. All procedures were in accordance with the Helsinki Declaration and informed consent of patients was waived because of the retrospective nature of the study. We identified 79 patients with surgically proven PanNETs from January 2020 to June 2023. In the definition of PanNETs grading, Grade 1 is with mitotic count < 2 per/2 mm^2 and < 3% Ki-67 index, grade 2 is with mitotic count with 2–20/2 mm^2 and 3–20% Ki-67 index whereas grade 3 is with mitotic count > 20/2 mm^2 and > 20% Ki-67 index. PanNECs patients were not included in the study. A flowchart of patient enrollment is shown in Fig. 1.

The inclusion criteria were: (1) patients with pathology-proven PanNETs; (2) patients underwent dynamic pancreatic imaging examination within 30 days prior to surgery; (3) patients with completeness of clinical data.

The exclusion criteria was: patients received any antitumor therapy before surgery. 21 patients were excluded as the following reasons: insufficient pathologic data ($n = 8$)

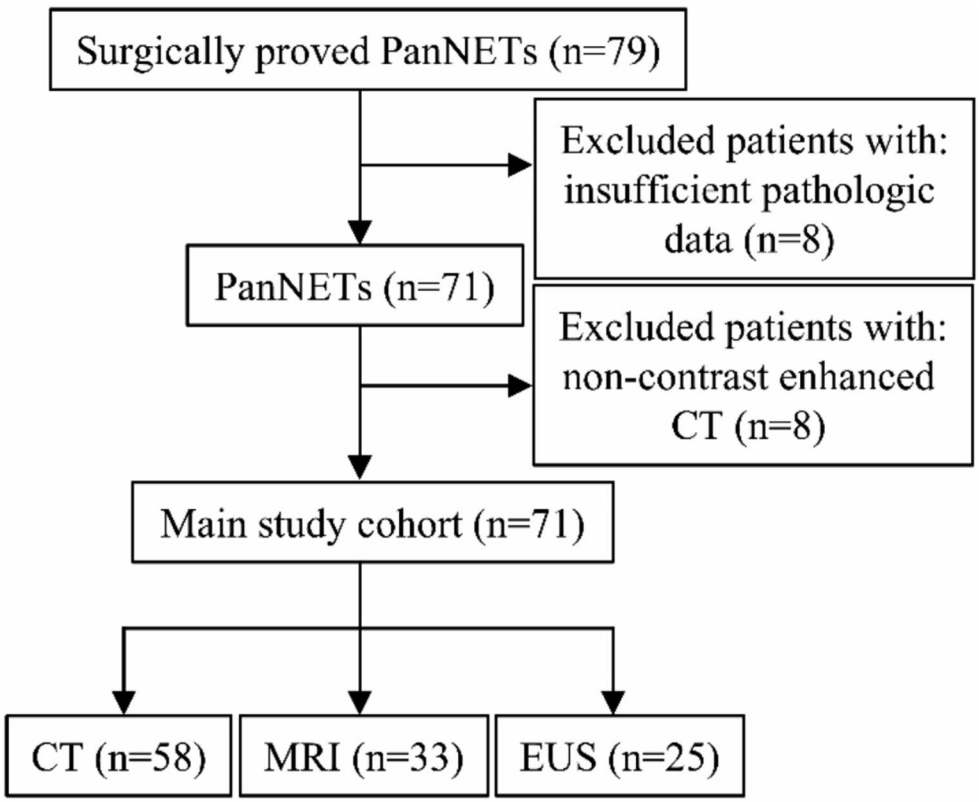

Fig. 1 Flowchart of patient selection. *PanNETs* pancreatic neuroendocrine tumors; *CT* computed tomography; *MRI* magnetic resonance imaging; *EUS* endoscopic ultrasonography

and non-contrast CT examinations ($n=13$). Finally, total of 58 patients were included in this study (Fig. 1).

CT image acquisition and feature analysis

All patients underwent CT scan on the supine multi detector spiral CT scanner (Lightspeed, VCT or discovery hd750, GE Healthcare, US) from the right diaphragm to the pubic symphysis. The following were CT scan parameters: tube voltage 120 kVp, tube current 250–350 mA, collimating slice thickness 5 mm, reconstruction slice thickness 1.25 mm, slice interval 5 mm, rotation time 0.6 s, helical pitch 1.375, the field of view between 35 and 40 cm, matrix 512 × 512. Simultaneously all the images used a standard reconstruction algorithm. As for enhanced CT scan, the patient's elbow vein was injected into a contrast agent (Omnipaque 350 mgI/mL, GE Healthcare, US) of 1.2 mL/kg per body weight at an injection rate of 3.0 mL/s and then 40 mL of saline solution was injected at the same injection rate. The arterial phase, portal vein phase and equilibrium phase images were obtained at 35 s, 70 s and 3 min after the injection of contrast agent. Circular or elliptical regions of interest (ROIs) were drawn to surround as much of the tumor as possible avoiding the calcification, vessels, and normal pancreas. Meanwhile, the ROI of normal pancreas near the lesion was measured. three adjacent images were measured and after that the results were averaged.

For all measurements, the size, shape, and position of the ROIs were kept constant between the two phases (arterial phase (AP) and portal phase (PP). All tumors were evaluated for: (a) tumor location (head, body, or tail of the pancreas), (b) size (the maximum diameter of the tumor in the cross section), (c) cystic changes within the tumor (solid or cystic-solid), (d) pancreatic duct dilatation (PDD) (>3 mm), (e) pancreatic atrophy, (f) calcification, (g) tumor margin (well defined [tumor margin smooth and clearly visible] or poorly defined [with spiculation or infiltration on >90° of the tumor perimeter]), (h) enhancement (homogenous or heterogeneous), (i) arterial enhancement ratio (AER, hounsfield units (HU) values of tumor/HU values of normal parenchyma measured on AP) and (j) portal enhancement ratio (PER, HU values of tumor/HU values of normal parenchyma measured on PP). The representative CT findings were shown in Fig. 2.

MRI image acquisition and feature analysis

MR scans were performed by using a 3.0-T or 1.5-T unit (Signa HDx 3.0-T; GE Medical Systems, Milwaukee, WI, United States, or Achieva 1.5-T; Philips, Amsterdam, The Netherlands) including conventional axial, sagittal, and coronal T1-weighted turbo spin-echo imaging sequence (without and with gadolinium), fast spin-echo T2-weighted fat-suppressed sequence (echo time/repetition time TE/TR: 4,000–8,000/80–90 ms); MRCP was performed by using heavily T2-weighted fast acquisition spin echo sequence (TR/TE: 2,400–6,000/500–800 ms). As for contrast enhanced imaging, the patient's elbow vein was injected into 0.1 mmol/kg gadolinium (2.5 ml/s).

All the images were assessed independently by two experienced radiologists, who were blinded to the PanNETs pathological grade. The tumor features were determined

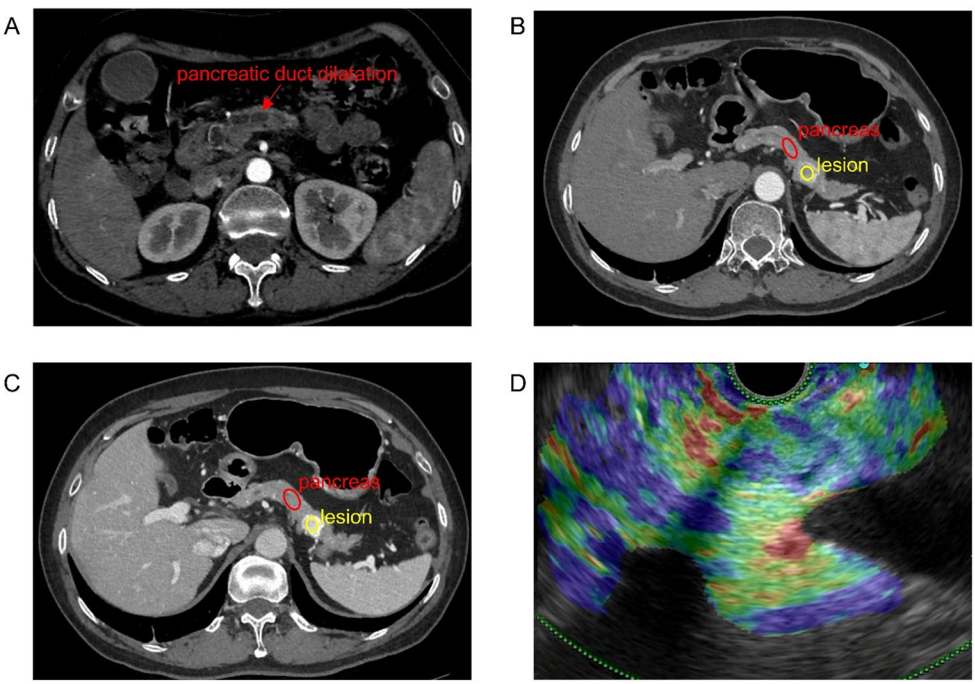

Fig. 2 Representative images of PanNETs imaging features. (**A**) Representative CT image of PanNETs grade 3 with pancreatic duct dilatation. (**B**) Region of interest placement on lesion and adjacent normal pancreas in an axial CT image of arterial phase of PanNETs grade 1. (**C**) Region of interest placement on lesion and adjacent normal pancreas in an axial CT image of portal phase of PanNETs grade 1. (**D**) Representative EUS image of PanNETs grade 1 evaluated for elastography score. *PanNETs* pancreatic neuroendocrine tumors; *CT* computed tomography; *EUS* endoscopic ultrasonography

based on the lesion signal intensity in (a) T1WI (hypointense, isointense), (b) T2WI (hypointense, isointense or hyperintense) and (c) DWI (moderate hyperintense or marked hyperintense).

EUS image acquisition and feature analysis

Before endoscopic or surgical resection, patients underwent EUS examinations after anesthesiologist conducted moderate sedation with fentanyl and propofol. EUS was performed by using radial echoendoscopes (GF-UM2000; Olympus Medical Systems, Tokyo, Japan) and/or linear echoendoscopes (UCT 260; Olympus Medical Systems, Tokyo, Japan), matching mainframe/ultrasound processing system (EU-M2000 and/or EU-ME2; Olympus Medical Systems, Tokyo, Japan) at frequencies of 6, 7.5, and 10 MHz. EUS examinations were conducted and evaluated by several experienced endoscopists which referred to doctors who had been practicing for at least 5 years and had conducted at least 200 EUS examinations every year.

All tumors were evaluated for elastography score. The scoring criteria were: 1, the image showed a homogenous soft tissue area (green) corresponding to normal tissue; 2, the image indicated heterogenous soft tissue (green, yellow, and red) corresponding to fibrosis or inflammatory tissue; 3, the image displayed mixed colors or a honeycombed elastography pattern indicative of mixed hard and soft tissue making the interpretation difficult; 4, the image displayed a small soft (green) central area surrounded by mainly hard (blue) tissue corresponding to a malignant hypervascularized lesion and 5 was assigned to lesions representing mainly hard (blue) tissue with areas of heterogeneous soft tissue (green, red) representing zones of necrosis in an advanced malignant lesions [19]. The representative EUS imaging was shown in Fig. 2.

Table 1 Patient demographics ($n=58$)

Characteristic	Value
Gender	
Male	35 (60.3%)
Female	23 (39.7%)
Age (y)	
Mean ± SD	56.9 ± 11.5
Tumor location	
Head	13 (25.9%)
Body or tail	45 (74.1%)
Tumor size (cm)	
Mean ± SD	2.6 ± 1.9
WHO grade	
1	29 (50.0%)
2	23 (39.7%)
3	6 (10.3%)

WHO world health organization; data in parentheses are percentages

Statistical analysis

The data were managed and analyzed by using SPSS 27.0 (IBM Corp., Armonk, NY, United States). Quantitative data were summarized as means ± SD and were analyzed by independent-samples t test. Categorical parameters were presented as absolute (frequencies) and statistical analysis was examined with Chi-square test or Fisher's exact test. Multivariable analyses for PanNETs grading were calculated with a logistic regression model. Variables with a P value < 0.05 in univariable analyses were included in multivariable analyses. The predictive efficiencies of different factors were calculated by using receiver operating characteristic (ROC) curves and the area under the ROC curve (AUC) by using MedCalc software (Mariakerke, Belgium). P value < 0.05 was considered as statistically significant.

Results

Patients' characteristics

A total of 58 patients with PanNETs in this study were diagnosed through surgical resection and pathological analysis. Among these patients, 29 patients (50.0%) were categorized as grade 1, 23 (39.7%) were grade 2, and 6 (10.3%) were grade 3 according to the WHO classification. Their characteristics are summarized in Table 1. There were 35 men and 23 women, and the mean age was 56.9 years. Additionally, the mean diameter of the lesions was 2.6 cm and 74.1% of the tumors were located in the body or tail and 25.9% in the head.

Clinical and radiological characteristics

The clinical characteristics, CT features and MRI features are summarized in Table 2. Significant differences were found in gender, tumor size, the presence or absence of PDD, tumor margin, AER and PER among PanNETs G1 and PanNETs G2/3 tumors (all $P<0.05$). PanNETs G2/3 usually occurred in female and showed larger size, higher rate of PDD and poorly defined margin compared with PanNETs G1. In addition, the AER and PER in PanNETs G2/3 were significantly lower than those in PanNETs G1. As for MRI finding, there were no significant differences in TIWI, T2WI and DWI signal intensity and enhancement heterogeneity between PanNETs G1and PanNETs G2/3.

CT features showing significant differences between PanNETs G2/3 and G1 were selected for multivariable logistic regression analysis, and the result showed that gender, PDD and PER are independent predictors for differentiating PanNETs G2/G3 from PanNETs G1 (Table 3).

Table 2 The summary of clinical characteristics, CT and MRI findings according to PanNETs grade ($n=58$)

Variables	WHO grade		*P* value
	G1	G2/3	
Gender			0.003*
Male	23	12	
Female	6	17	
Age (y)	57.9 ± 11.1	55.8 ± 12.0	0.491
Tumor location			0.354
Head	8	5	
Body or tail	21	24	
Tumor size (cm)	1.82 ± 1.11	3.31 ± 2.29	0.003*
CT			
Cystic	0	0	0.578
Solid	21	19	
Cystic-solid	8	10	
PDD			0.009*
Yes	2	10	
No	27	19	
Pancreatic atrophy			0.723
Yes	4	5	
No	25	24	
Calcification			0.693
Yes	4	3	
No	25	26	
Tumor margin			0.035*
Well defined	20	12	
Poorly defined	9	17	
Enhancement			0.294
Homogeneous	19	15	
Heterogeneous	10	14	
AER	1.50 ± 0.51	1.12 ± 0.49	0.006*
PER	1.40 ± 0.38	0.99 ± 0.34	<0.001*
MRI			
T1WI			0.248
Hypointense	14	12	
Isointense	2	5	
T2WI			0.327
Hypointense	2	4	
Isointense	1	2	
Hyperintense	13	11	
DWI			0.784
Moderate hyperintense	12	12	
Marked hyperintense	4	5	

WHO world health organization; *CT* computed tomography; *PDD* pancreatic duct dilation; *AER* arterial enhancement ratio; *PER* portal enhancement ratio; *MRI* magnetic resonance imaging

EUS findings

Considering that there are fewer PanNETs patients undergoing EUS, we conducted a univariate analysis individually of the elastography scores of 25 patients and found a significant difference in elastography scores between G1 and G2/3, with G2/3 patients having higher scores (Table 4).

Table 3 Multivariate analysis for differentiating PanNETs G2/G3 from PanNETs G1

Variables	Odds ratio	95%CI	*P* value
Gender (Male vs. Female)	0.079	0.013–0.493	0.007*
Tumor size (cm)	1.613	0.908–2.866	0.103
PDD (Yes vs. No)	15.602	1.016-239.697	0.049*
Tumor margin (Poorly vs. Well)	2.741	0.455–16.497	0.271
AER	2.988	0.158–56.671	0.466
PER	0.008	0-0.788	0.039*

PDD Pancreatic duct dilation; *AER* Arterial enhancement ratio; *PER* Portal enhancement ratio

Table 4 The comparison of elastography scores between PanNETs G1 and PanNETs G2/3

Variables	WHO grade		*P* value
	G1 ($n=11$)	G2/3 ($n=14$)	
Elastography score	2.36 ± 0.51	3.50 ± 0.94	0.001*
2	7	2	
3	4	5	
4	0	5	
5	0	2	

WHO world health organization

Predictive performances of clinical and imaging findings for pannets

Subsequently, the predictive performances of the above indicators in differentiating PanNETs G2/G3 from PanNETs G1 were compared on the basis of ROC curves. The AUC of gender, PDD and PER was 0.690 (95% confidence interval [CI], 0.551–0.828), 0.638 (95% CI, 0.494–0.782) and 0.791 (95% CI, 0.673–0.909) respectively. To improve the predictive accuracy, we tested the combination of gender, PDD and PER for PanNETs grading. Notably, using the combination significantly improved the predictive efficiency in differentiating patients with PanNETs G2/G3 from those with PanNETs G1 when compared to these three variables alone, with an AUC of 0.925 (95% CI, 0.825–0.978). In addition, the AUC of the elastography score was 0.838 (95% CI, 0.680–0.995) (Fig. 3; Table 5). The ROC curve analysis also showed that the optimal cut-off value of PER and elastography score for PanNETs grading was 1.23 and 3.0.

Discussion

The pathological grade of PanNETs was significantly related to the treatment and prognosis of patients. Different treatment measures will seriously affect the survival of patients [20]. Preoperative full understanding of the pathological grade of patients' tumors plays an important role in the selection of surgical methods [21]. In this study, three

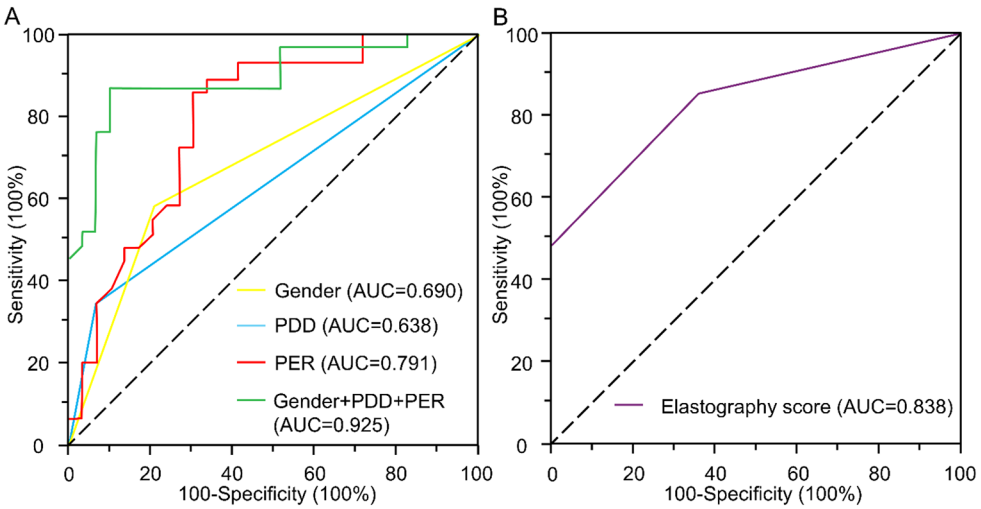

Fig. 3 ROC curve analysis of gender, PDD, PER (**A**) and elastography score (**B**) for differentiating PanNETs G2/G3 from PanNETs G1. *ROC* receiver operating characteristic; *PDD* pancreatic duct dilation; *PER* portal enhancement ratio; *PanNETs* pancreatic neuroendocrine tumors; *AUC* the area under the ROC curve

Table 5 Predictive efficiencies of different variables in differentiating patients with PanNETs G2/3 and PanNETs G1

Variables	Sensitivity (%)	Specificity (%)	95%CI	AUC	*P* value
Gender	58.6	79.3	0.551–0.828	0.690	0.0016*
PDD	54.5	93.1	0.494–0.782	0.638	0.0067*
PER	86.2	69.0	0.673–0.909	0.791	<0.001*
Gender+PDD+PER	86.2	93.1	0.825–0.978	0.925	<0.001*
Elastography score	50.0	100.00	0.680–0.995	0.838	<0.001*

PDD pancreatic duct dilatation; *PER* portal enhancement ratio; *CI* confidence interval; *AUC* the area under the receiver operating characteristic curve

imaging modalities were used to establish the preoperative prediction model of pathological grade of PanNETs: CT, MRI, and EUS. Considering that EUS is an invasive examination which has not been routinely included before 2022 at our institution, the number of patients who underwent EUS was relatively small ($n=25$), we performed a separate univariate analysis of elastography scores of EUS.

In the present study, based on the clinical characteristics, CT and MRI findings, univariate logistic regression analysis showed that gender, tumor diameter, PDD, tumor margin, AER and PER were significantly different between patients with PanNETs G1 and G2/3 ($P<0.05$). By multivariate analysis, gender, PDD and PER were predictive factors for pathological grade of PanNETs. In the analysis of the predictive efficiencies of these factors, female (AUC=0.690), PDD (AUC=0.638) and low PER (AUC=0.791) showed a great performance of prediction of PanNETs G2/3. Meanwhile, the predictive efficiency was significantly improved when these variables were combined (AUC=0.925). In addition, there was also a significant difference in elastography score between PanNETs G1 and G2/3, and the AUC was 0.838, which indicated that EUS could effectively distinguish PanNETs G1 from G2/3.

Previous studies have highlighted the significant potential of radiomics in predicting the preoperative pathological grade of PanNETs. A single-centered study found an interpretable radiomics-based random forest model which can effectively differentiate between G1 and G2/3 of PanNETs, demonstrating favorable interpretability [18]. A recent study proposed a comprehensive nomogram consisting of tumor margin and fusion radiomic signature as a powerful tool to predict grade 1 and grade 2/3 PanNETs preoperatively and assist the clinical decision-making for PanNETs patients [22]. Another study showed that the maximum intensity feature can help to identify the G1 PanNETs from G2 PanNETs on the arterial phase images of MRI, which may be also applied to early recurrence or progression after surgical resection of PanNETs in the further study [23]. But radiomics has certain limitations. First, the sample size of most radiomics studies is small which may reduce the credibility of the results. Second, these studies are mostly single-centered studies and lack reliable external validation. Finally, the inconsistency of radiomics feature selection in different studies weakens the trust in these models [24]. Therefore, it may be a more direct way to predict the pathological grade of PanNETs preoperatively through imaging examination.

A previous study indicated significant difference was found in PDD among PanNETs G1, G2, and PanNECs G3 tumors ($P<0.05$) [25]. Canellas et al. found that tumors with PDD were six times more likely to develop intermediate or high grade tumors than tumors without PDD [26]. Another study including 94 patients with PanNETs found that PDD may help to identify different pathological grade of PanNETs [27]. For the result that G2/3 are more likely to cause PDD, the reasons are as follows: first, PanNETs G2/3 may have a larger volume, as showed in our study, which is

easy to compress the pancreatic duct and cause obstruction. Second, it may be because the tumor extensive fibrosis in the cytoplasm and around the lesion caused obstruction by pulling the catheter. Finally, G2/3 PanNETs are more invasive, and have a certain chance to invade the pancreas, duodenum and biliary system which cause PDD.

The PER was defined as the portal tumor HU value divided by the adjacent parenchyma HU value on the same phase [28]. In a single-center study that included 94 patients with PanNETs, PER had the highest AUC for quantitative characteristics at 0.855 [29]. Another recent study found that the tumor-pancreas enhancement ratio in the portal stage reliably identified tumors in all cases of G3 [30]. It is reported that the tumor PER reflects microvascular density (MVD), and the MVD is also found to be low in PanNETs G3. Therefore, it is possible and reasonable to predict the pathological grade by AER and PER [31]. All these features were addressed in the present study, showing significant predictive value, which is similar to the previously reported results.

MRI has been shown to be of great value in detecting and characterizing PanNETs as well as detecting liver metastases. MRI and contrast-enhanced scan clearly showed the size, shape, enhancement characteristics of pancreatic lesions and the extent of PDD [32]. In terms of predicting pathological grade, Guo and Toshima et al. showed there were no significant differences in T1WI/T2WI signal intensity and enhancement heterogeneity between patients with different grades of PanNETs [33, 34]. This is consistent with our results, suggesting that the predictive efficacy of T1WI/T2WI for grading PanNETs is low. Although there was no difference in DWI between PanNETs G1 and PanNETs G2/3 in our results, some studies have shown the effectiveness of predicting pathological grade by apparent diffusion coefficient (ADC) values of the tumor in DWI [35], and in the future we may need to expand the sample size for further validation.

EUS is usually applied to the preoperative diagnosis of PanNETs rather than pathological grading. A recent study reported that some features of EUS like well-defined margins, vascularization, hypoechoic appearance, and the presence of a hypoechoic rim were significantly associated with PanNETs diagnosis [14]. Elastography in EUS usually indicates the appearance of focal pancreatic lesions, which is characterized by uneven, mainly blue, with small green and red areas. A more uniform blue pattern is more typical in PanNETs [36]. Our result showed that PanNETs G2/3 had higher elastography scores than G1 which revealed that elastography score can be used as a predictor of preoperative pathological grade of PanNETs. The effect of gender on the pathological grade of PanNETs is currently controversial, with most studies suggesting that there are no differences in gender in patients with different grades of PanNETs [37]. The result that females are more likely to suffer from PanNETs G2/3 may be related to the small sample size of our institution and need to be validated by larger sample size.

However, this study has some limitations, which must be taken into account when interpreting the results. First, this is a single center-based retrospective study. Second, the number of patients is small, with only 6 cases of PanNETs G3. Considering that PanNETs is a relatively rare type of pancreatic tumor, the number of patients in this study is acceptable from the data published in the literature. Finally, we have not further distinguished G2 and G3, which may not be enough to clarify the usefulness of the model. Further large-scale and prospective studies are needed to clearly evaluate the role of these indicators in PanNETs classification prediction.

In conclusion, we confirmed the effectiveness of the combination of contrast-enhanced CT and EUS in predicting the preoperative pathological grade of PanNETs in this study. Combining gender, PDD, PER and elastography score can improve the accuracy of preoperative prediction of PanNETs grade.

Supplementary Information The online version contains supplementary material available at https://doi.org/10.1007/s00261-025-04865-4.

Author contributions All authors attest that they meet the current International Committee of Medical Journal Editors (ICMJE) criteria for Authorship. All authors have contributed to, read and approved the final version of the manuscript. The detailed Authors' contributions are described below: YX, EA, SZ, HBL, HHX, QL YDQ and HC contributed to conceptualization; YX, EA and SZ contributed to method ology and formal analysis; YX, HBL and HHX contributed to writing original draft preparation; QL, YDQ and HC contributed to writing review and editing; HC contributed to supervision. Yu Xie, Elyar Abaydulla Elyar and Song Zhang are co-first authors. Yudong Qiu and Hao Cheng contributed equally as the co-corresponding authors.

Funding This project was supported by fundings for Clinical Trials from the Affiliated Drum Tower Hospital, Medical School of Nanjing University (No.2023-LCYJ-PY-15 and No.2022-LCYJ-PY-45).

Data availability No datasets were generated or analysed during the current study.

Declarations

Ethical approval Institutional review board approval was obtained.

Informed consent Written informed consent was waived by the Institutional Review Board.

Competing interests The authors declare no competing interests.

References

1. Dasari A, Shen C, Halperin D, et al (2017) Trends in the Incidence, Prevalence, and Survival Outcomes in Patients With Neuroendocrine Tumors in the United States. JAMA Oncol 3: 1335–1342
2. Nagtegaal ID, Odze RD, Klimstra D, et al (2020) The 2019 WHO classification of tumours of the digestive system. Histopathology 76: 182–188
3. Lam AK, Ishida H, (2021) Pancreatic neuroendocrine neoplasms: Clinicopathological features and pathological staging. Histol Histopathol 36: 367–382
4. Ohmoto A, Rokutan H, Yachida S, (2017) Pancreatic Neuroendocrine Neoplasms: Basic Biology, Current Treatment Strategies and Prospects for the Future. Int J Mol Sci 18
5. Liu X, Chen B, Chen J, et al (2023) The incidence, prevalence, and survival analysis of pancreatic neuroendocrine tumors in the United States. J Endocrinol Invest 46: 1373–1384
6. Cives M, Strosberg JR, (2018) Gastroenteropancreatic Neuroendocrine Tumors. CA Cancer J Clin 68: 471–487
7. Juchems M, Kläsner B, (2023) [Neuroendocrine tumors of the pancreas]. Radiologie (Heidelb) 63: 894–899
8. Luo Y, Chen X, Chen J, et al (2020) Preoperative Prediction of Pancreatic Neuroendocrine Neoplasms Grading Based on Enhanced Computed Tomography Imaging: Validation of Deep Learning with a Convolutional Neural Network. Neuroendocrinology 110: 338–350
9. Luo Y, Chen J, Huang K, et al (2017) Early evaluation of sunitinib for the treatment of advanced gastroenteropancreatic neuroendocrine neoplasms via CT imaging: RECIST 1.1 or Choi Criteria? BMC Cancer 17: 154
10. Liang W, Yang P, Huang R, et al (2019) A Combined Nomogram Model to Preoperatively Predict Histologic Grade in Pancreatic Neuroendocrine Tumors. Clin Cancer Res 25: 584–594
11. Chiti G, Grazzini G, Cozzi D, et al (2021) Imaging of Pancreatic Neuroendocrine Neoplasms. Int J Environ Res Public Health 18
12. Manta R, Nardi E, Pagano N, et al (2016) Pre-operative Diagnosis of Pancreatic Neuroendocrine Tumors with Endoscopic Ultrasonography and Computed Tomography in a Large Series. J Gastrointestin Liver Dis 25: 317–321
13. Sun H, Zhou J, Liu K, et al (2019) Pancreatic neuroendocrine tumors: MR imaging features preoperatively predict lymph node metastasis. Abdom Radiol (NY) 44: 1000–1009
14. Saizu I, Cotruta B, Iacob RA, et al (2023) A MODEL TO PREDICT DIAGNOSIS OF PANCREATIC NEUROENDOCRINE TUMORS BASED ON EUS IMAGING FEATURES. Acta Endocrinol (Buchar) 19: 407–414
15. Chen Y, Huang F, Fan Y, et al (2022) Diagnostic value of endoscopic ultrasound for detecting pancreatic neuroendocrine tumors: A systematic review and meta-analysis. Am J Med Sci 363: 511–518
16. Crinò SF, Ammendola S, Meneghetti A, et al (2021) Comparison between EUS-guided fine-needle aspiration cytology and EUS-guided fine-needle biopsy histology for the evaluation of pancreatic neuroendocrine tumors. Pancreatology 21: 443–450
17. Di Leo M, Poliani L, Rahal D, et al (2019) Pancreatic Neuroendocrine Tumours: The Role of Endoscopic Ultrasound Biopsy in Diagnosis and Grading Based on the WHO 2017 Classification. Dig Dis 37: 325–333
18. Ye JY, Fang P, Peng ZP, et al (2024) A radiomics-based interpretable model to predict the pathological grade of pancreatic neuroendocrine tumors. Eur Radiol 34: 1994–2005
19. Giovannini M, Thomas B, Erwan B, et al (2009) Endoscopic ultrasound elastography for evaluation of lymph nodes and pancreatic masses: a multicenter study. World J Gastroenterol 15: 1587–1593
20. Hofland J, Falconi M, Christ E, et al (2023) European Neuroendocrine Tumor Society 2023 guidance paper for functioning pancreatic neuroendocrine tumour syndromes. J Neuroendocrinol 35: e13318
21. Ma ZY, Gong YF, Zhuang HK, et al (2020) Pancreatic neuroendocrine tumors: A review of serum biomarkers, staging, and management. World J Gastroenterol 26: 2305–2322
22. Gu D, Hu Y, Ding H, et al (2019) CT radiomics may predict the grade of pancreatic neuroendocrine tumors: a multicenter study. Eur Radiol 29: 6880–6890
23. Li W, Xu C, Ye Z, (2021) Prediction of Pancreatic Neuroendocrine Tumor Grading Risk Based on Quantitative Radiomic Analysis of MR. Front Oncol 11: 758062
24. Bezzi C, Mapelli P, Presotto L, et al (2021) Radiomics in pancreatic neuroendocrine tumors: methodological issues and clinical significance. Eur J Nucl Med Mol Imaging 48: 4002–4015
25. Guo C, Zhuge X, Wang Z, et al (2019) Textural analysis on contrast-enhanced CT in pancreatic neuroendocrine neoplasms: association with WHO grade. Abdom Radiol (NY) 44: 576–585
26. Canellas R, Burk KS, Parakh A, et al (2018) Prediction of Pancreatic Neuroendocrine Tumor Grade Based on CT Features and Texture Analysis. AJR Am J Roentgenol 210: 341–346
27. Huang J, Chen J, Xu M, et al (2021) Contrast-Enhanced Ultrasonography Findings Correlate with Pathologic Grades of Pancreatic Neuroendocrine Tumors. Ultrasound Med Biol 47: 2097–2106
28. Chen HY, Pan Y, Chen JY, et al (2022) Quantitative analysis of enhanced CT in differentiating well-differentiated pancreatic neuroendocrine tumors and poorly differentiated neuroendocrine carcinomas. Eur Radiol 32: 8317–8325
29. Xu W, Yan H, Xu L, et al (2020) Correlation between radiologic features on contrast-enhanced CT and pathological tumor grades in pancreatic neuroendocrine neoplasms. J Biomed Res 35: 179–188
30. D'Onofrio M, Ciaravino V, Cardobi N, et al (2019) CT Enhancement and 3D Texture Analysis of Pancreatic Neuroendocrine Neoplasms. Sci Rep 9: 2176
31. Horiguchi S, Kato H, Shiraha H, et al (2017) Dynamic computed tomography is useful for prediction of pathological grade in pancreatic neuroendocrine neoplasm. J Gastroenterol Hepatol 32: 925–931
32. Xu W, Zhang H, Feng G, et al (2021) The value of MRI in identifying pancreatic neuroendocrine tumour G3 and carcinoma G3. Clin Radiol 76: 551.e551-551.e559
33. Guo C, Chen X, Xiao W, et al (2017) Pancreatic neuroendocrine neoplasms at magnetic resonance imaging: comparison between grade 3 and grade 1/2 tumors. Onco Targets Ther 10: 1465–1474
34. Toshima F, Inoue D, Komori T, et al (2017) Is the combination of MR and CT findings useful in determining the tumor grade of pancreatic neuroendocrine tumors? Jpn J Radiol 35: 242–253

35. De Robertis R, Cingarlini S, Tinazzi Martini P, et al (2017) Pancreatic neuroendocrine neoplasms: Magnetic resonance imaging features according to grade and stage. World J Gastroenterol 23: 275–285
36. Janssen J, Schlörer E, Greiner L, (2007) EUS elastography of the pancreas: feasibility and pattern description of the normal pancreas, chronic pancreatitis, and focal pancreatic lesions. Gastrointest Endosc 65: 971–978
37. Ma J, Wang X, Tang M, et al (2024) Preoperative prediction of pancreatic neuroendocrine tumor grade based on (68)Ga-DOTATATE PET/CT. Endocrine 83: 502–510